An Improved Direct Torque Control of Induction Machines

N. R. N. Idris, *member IEEE*, and A. H. M. Yatim, *member, IEEE*

Abstract--**The direct torque control (DTC) of induction machines with conventional hysteresis comparators suffer from variable switching frequency. This is simply because of the variable torque slope which depends on the operating conditions. An innovative, simple and new torque controller which can offer a constant torque switching frequency is proposed. To further improved the performance of the DTC drive, a simple stator flux compensator is also proposed. The compensator corrects the steady state stator flux phase and magnitude errors and thus improve on the torque estimation and drive performance. Simulation and experimental results are presented to validate the proposed schemes.**

Index Terms—**AC motor drives, torque control, induction motor drives.**

I. Introduction

More than a decade ago, direct torque control (DTC) was introduced to give a fast and good dynamic torque response and can be considered as an alternative to the field oriented control (FOC) technique[1,2]. The DTC scheme is very simple; it consists of DTC controller, torque and flux calculator, and VSI. The configuration is much simpler than the FOC system due to the absence of frame transformer, pulse width modulator and position encoder, which introduce delays and requires mechanical transducer. The DTC controller comprises of selection table and hysteresis comparator, which are relatively easy to implement.

The DTC drives which are based on hysteresis comparators, results in variable switching frequency due to the hysteresis comparators used for the torque and flux comparators. Several techniques have been proposed to overcome this problem, i.e to obtain a constant switching frequency. These include the use of predictive control technique[3,4], space vector modulation (SVM)[5] and artificial intelligence technique [6,7]. These techniques have somehow increases the complexity of the DTC drives which is known to have a simple control structure. A simple and more practical method in solving these problems is therefore necessary in order to maintain the simple control structure of DTC. This paper proposes simple yet effective method to maintain a constant switching frequency, that is by using a constant switching frequency torque controller.

It is shown that stator flux estimation based on voltage model will produce magnitude and phase errors. The phase error can results in a steady state torque ripple at 6 times the synchronous speed. The paper propose a method to improve the steady state performance of the voltage model based stator flux estimation thus minimises the steady state torque ripple. The outline of the paper is as follows. Section II describes the characteristics of hysteresis based torque controller in DTC and also the phase and magnitude errors caused by voltage model based stator flux estimation techniques and its effect on DTC drive. Section III gives the proposed technique for constant switching and improved stator flux estimation. Some simulation and experimental results are given in section IV and finally section V presents the conclusions.

N. R. N. Idris and A. H. M. Yatim are with the Department of Electrical Energy Conversion, Fakulti Kejuruteraan Elektrik, Universiti Teknologi Malaysia, 81310 UTM, Skudai, Johor, MALAYSIA (telephone: 607-550-5141, e-mail: nikrumzi@ ieee.org and halim@ieee.org).

II. DTC of Induction Machines

The simple structure of DTC is mainly due to its hysteresis based comparator and stator flux estimation technique which is based on voltage model. The switching pattern of the VSI is selected based on the output of a pair of hysteresis comparators for the torque and flux. Since the torque and flux errors are limited within their hysteresis bands, an independent control of torque and flux can be established. Although simple in structure, the hysteresis based comparator results in variable switching frequency and increased torque ripple. Voltage model of stator flux estimation which can be easily implemented poses problems due to the errors in magnitude and phase – this in turn

A. Torque controller based on hysteresis comparator

For precise position control application, particularly at low speed, it is necessary for the drive to produce a low electromagnetic torque ripple. As shown by [8], the torque ripple is only affected by the toque hysteresis band and is independent of the flux hysteresis band. It is also highlighted in [8] that the relation between the torque hysteresis band and the torque dispersion is linear. Owing to the digital implementation, and the delay that exist between the instance the variables are sampled and the instance the voltage switching pattern is determined and pass to the inverter, there is an overshoot or undershoot in the electromagnetic torque above or below the torque hysteresis bands; this results in a non-zero ripple even a zero torque hysteresis band is applied. In three level torque hysteresis implementation, the width of the hysteresis

0-7803-7233-6/01/$10.00 ©2001 IEEE.

torque band must be selected appropriately. If the band is too small, a torque overshoot which may cause the torque error to exceed the hysteresis band will occur [9]. This will result in a reverse voltage vector to be selected (instead of zero vector) to reduce the torque. A reverse voltage vector will reduce the torque rapidly and hence may in turn cause a torque undershoot. Therefore, the torque ripple can become high if the torque hysteresis band is set too small. Fig. 1. illustrate the scenario in which an overshoot in torque (undershoot in torque error) occurs which increases the torque ripple when the torque band is set too small. The undershoot in torque will also cause an increase in torque hysteresis comparator switching hence the average device switching.

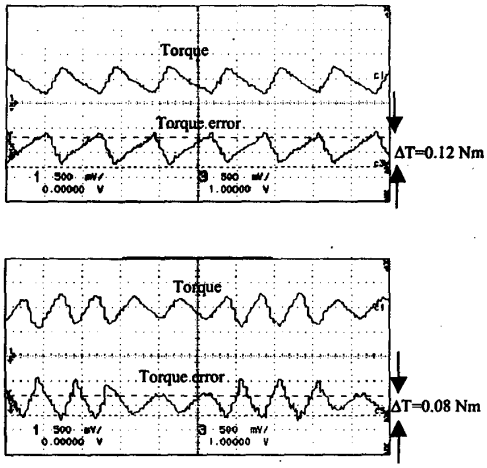

Fig. 1 Torque and torque error obtained from experimental results (a) Torque overshoot which does not exceed the hysteresis band, torque band = 0.12Nm (b) Torque overshoot which does exceed the hysteresis band, torque band = 0.08Nm

The average device switching frequency is mainly determined by the switching frequency of the torque hysteresis comparator. The positive and negative slope of the torque (slope$^+$ and slope$^-$) depends on the operating conditions, namely, the speed, stator and rotor fluxes, and stator voltage vectors as given by equations (1) and (2).

$$slope^+ \equiv \frac{T_{e,n+1}-T_{e,n}}{t_s} = -\frac{T_{e,n}}{\sigma\tau_{sr}} + \frac{3p}{4}\frac{L_m}{\sigma L_s L_r}\left[(\bar{v}_s - j\omega_r\bar{\psi}_s)\cdot j\bar{\psi}_r\right] \quad (1)$$

$$slope^- \equiv \frac{T_{e,n+1}-T_{e,n}}{t_s} = -\frac{T_{e,n}}{\sigma\tau_{sr}} + \frac{3p}{4}\frac{L_m}{\sigma L_s L_r}\left[(-j\omega_r\bar{\psi}_s)\cdot j\bar{\psi}_r\right] \quad (2)$$

Where, $1/(\sigma\tau_{sr}) = \frac{R_s}{\sigma L_s} + \frac{R_r}{\sigma L_r}$

Since the torque slope determine how fast the torque touches its upper and lower bands, the average switching frequency is affected by the slope and hence the operating conditions. The torque band therefore has be adjusted to such that in worst case condition, the maximum switching frequency of the device is not exceeded. This means that the operation of the hysteresis comparator is not optimised for other conditions.

B. Torque ripple due to phase error in stator flux estimator

It is a common practice to replace a pure integrator in the voltage model-based estimator with a low pass filter (LP filter) in order to avoid integration drift problems. However doing so will result in a phase and magnitude errors present in the estimated stator flux. The phase error between the estimated and actual stator flux can be shown to cause the undesirable harmonic torque ripple at six times the synchronous frequency [9]. Thus in order to minimise the ripple phase error which is due to the LP filtering action has to be compensated.

III. Proposed Methods to Improve DTC Performance

The proposed methods discussed in this section are divided in to parts: to maintain the constant switching frequency and to improve the stator flux estimation hence to minimise the steady state torque ripple.

A. Constant switching frequency controller

The proposed torque controller consists of two triangular waveform generators, two comparators and a PI controller as shown in Fig. 1. The two triangular waveforms (which will be referred to as upper and lower carriers), are 180° out of phase with each other. The absolute values of the DC offsets for upper and lower carriers are set to half of its peak-peak value; the upper dc offset is positive while the lower is negative. In principle, the output of the proposed torque controller is similar to that of the three level hysteresis comparator [1], which can be either of three states: −1 , 0 or 1.

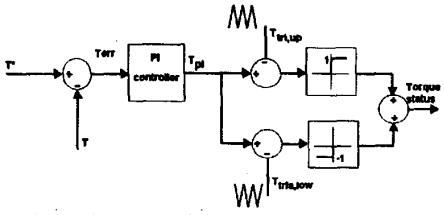

Fig. 2 Proposed torque controller

The value of the instantaneous output of the torque controller – named as *torque error status* and designated by *q(t)* is given by :

$$q(t)=\begin{cases} 1 \ for\ T_{pi} \geq C_{upper} \\ 0 \ for\ C_{lower} < T_{pi} < C_{upper} \\ -1 \ for\ T_{pi} \leq C_{lower} \end{cases} \quad (3)$$

The average torque error status, $\bar{q}(t)$, is defined as *continuous duty ratio* and is denoted by d(t). The average is taken over an interval T_{tri}, which is the period of the trangular carrier waveform. It is defined by

$$d(t)=\frac{1}{T_{tri}}\int_{t}^{t+T_{tri}} q(t)\,dt \quad (4)$$

The values of the PI controller parameters are chosen based on the linear analysis of the controller in Fig. 1. The linear model is obtained by averaging and linearising the torque equations (1) and (2). It can be shown that [10] the positive and negative torque slope equations are given by (5) and (6) respectively:

$$\frac{dT_e^+}{dt}=-AT_e+Bv_s^{\psi s}+K_1\left(\frac{\omega_e}{d}-\omega_r\right) \quad (5)$$

$$\frac{dT_e^-}{dt}=-AT_e-K_1\omega_r \quad (6)$$

where

$$A=\frac{1}{\sigma\tau_{sr}}$$

$$B=\frac{3p}{4}\frac{L_m}{\sigma L_s L_r}\psi_s$$

$$K_1=\frac{3p}{4}\frac{L_m}{\sigma L_s L_r}(\psi_s\psi_r^{\psi s})$$

Averaging and linearising equations (5) and (6), and with further simplifications, it can be shown that [9],

$$\frac{dT_e}{dt}=-AT_e+Bv_s^{\psi s}d+K_1(\omega_{slip}) \quad (7)$$

Based on (7), the transfer function between d and T_e can be obtained by setting the slip frequency to zero. It can also be shown that the transfer function between the output of the PI controller, T_{pi} and the averaged duty ratio d is given by a reciprocal of the peak-peak triangular carrier, C_{pp}. Thus the overall small signal block diagram of the proposed torque controller of Fig. 2 with averaged, linearised torque equation is shown in Fig. 3

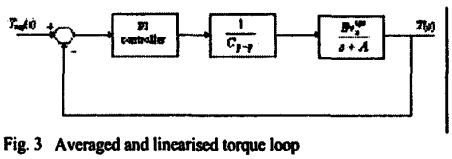

Fig. 3 Averaged and linearised torque loop

The values of the PI controller's parameters are chosen based on the following constraints:

- The absolute slope of equation (5) and (6) cannot exceed the triangular carrier slope
- The cross-over frequency of the loop gain of Fig. 3 (bandwidth) cannot exceed half of the carrier triangular frequency.

With these constraints and the motor parameters given in appendix, the parameters for the PI controller are chosen as:

$$K_p = 330 \quad \text{and} \quad K_i = 112826$$

B. Improved stator flux estimation

Stator flux estimation based on voltage model is estimated by using equation (8)

$$\bar{\Psi}_s=\int(\bar{v}-\bar{i}_s R_s)dt \quad (8)$$

With a low-pass filter, sinusoidal steady state form, it can be shown that:

$$\bar{\Psi}'_s=\frac{\bar{V}_s-\bar{I}_s R}{j\omega_e+\omega_c} \quad (9)$$

Where ω_c is the cut-off frequency of the low-pass filter in rad/s and Ψ_s' is the estimated stator based on LP filter. For a synchronous frequency larger than the cut-off, equation (9) can be graphically visualized using a phasor diagram as shown in fig. 4.

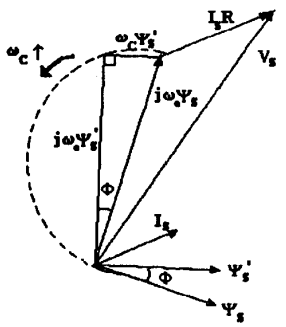

Fig. 4. Phasor diagram for steady state operation of induction machine showing the actual and estimated stator flux based on LP filter.

If $\bar{\Psi}'_s=\Psi'_s\angle\theta'$ and $\bar{\Psi}_s=\Psi_s\angle\theta$, then it can be shown that the relation between the estimated stator flux based on LP filter and pure integrator is given by (10):

$$\frac{\Psi'_s}{\Psi_s}\angle\theta'-\theta=\frac{\omega_e}{\sqrt{\omega^2{}_e+\omega^2{}_c}}\angle\phi \quad (10)$$

where $\phi=\pi/2-\tan^{-1}(\omega_e/\omega_c)$

The core of the proposed improvement is to provide a magnitude and phase compensations for the estimated flux, under steady state condition, only at the operating frequency thus improving the steady state performance of the DTC drive. In other words, the LP filter action is effective at all frequency except at the operating frequency, that is,

$$\psi_s' = \begin{cases} \dfrac{v - iR}{j\omega} & for \ \omega = \omega_e \\ \dfrac{v - iR}{j\omega + \omega_c} & for \ \omega \neq \omega_e \end{cases} \quad (11)$$

The LP filter action is therefore valid or effective for the DC offsets and low frequency components present in the sensed currents or voltages. This avoids the integration drift problem while maintaining good system stability. This is due to the fact that the phase and magnitude errors are compensated at the operating frequency. The stator flux is compensated at the operating frequency for the *d* and *q* components by determining the expressions for the actual stator flux in terms of estimated stator flux in the stationary reference frame. Fig. 5 shows the relationship of the estimated and actual stator flux with their *d* and *q* components in the stationary reference frame, denoted by the direct and quadrature axis , d^s and q^s.

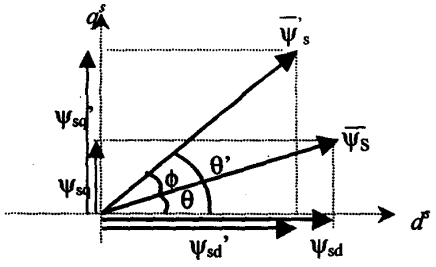

Fig. 5 The d and q components of the estimated and actual stator flux in stationary reference frame

In order to compensate for the error in the d and q axis of the estimated flux, the difference between the actual and estimated flux is added to the estimated flux and it can be shown that this is given by (2) and (13) and can be incorporated in the flux estimator block diagram as shown by Fig 6. The compensator can be initiated by the flag manually or based on steady state speed error.

$$\Psi_{sq} = \left(\Psi_q' - \Psi_d' \frac{\omega_c}{\omega_e} \right) \quad (12)$$

$$\Psi_{sd} = \left(\Psi_d' + \Psi_q' \frac{\omega_c}{\omega_e} \right) \quad (13)$$

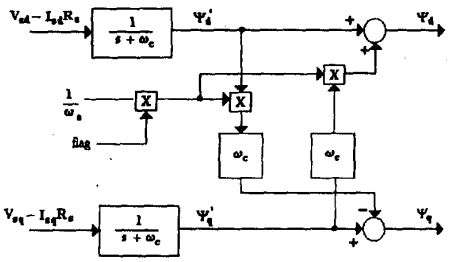

Fig 6. Block diagram of the improved stator flux estimator

The synchronous speed is ω_e is obtained from the measured terminal variables using (14).

$$\omega_e = -\frac{\left(\bar{v}_s - \bar{i}_s R_s\right)}{\Psi_s^2} \cdot j\overline{\Psi}_s \quad (14)$$

IV. Simulation and Experimental Results

Simulation as well as experiments were carried out to verify the viability of the proposed methods. The simulation was carried out using Matlab/Simulink while the experiment was carried out with the set up consisting of dSPACE controller card based on TMS320C31 DSP, IGBT VSI, standard ¼ HP induction machine coupled to a DC machine, and Xilinx FPGA to implement the voltage selection table and blanking time of the VSI. The block diagram of the experiment set-up is shown in Fig. 7

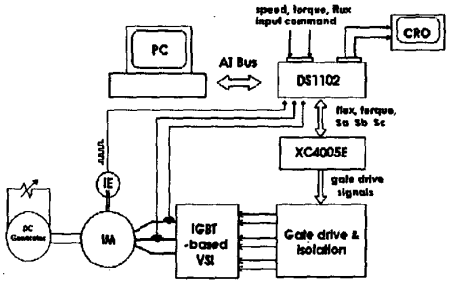

Fig. 7 Experiment Set-up

A. Constant switching frequency

The controller of Fig. 2 is implemented within the software with the sampling period of 55μs. The frequency spectrum of the phase currents at rotor speed of 10 and 70 rad/s for both the conventional hysteresis and proposed torque controller are shown in Fig. 8. It can be seen that the proposed controller has managed to maintain the dominant harmonics of the phase current at the triangular frequency regardless of the rotor speed., i.e. at about 2.3 kHz.

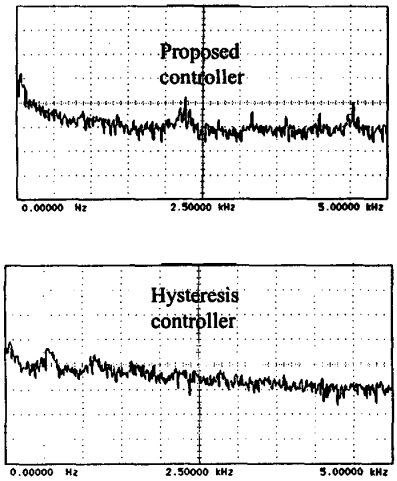

Fig. 8 Frequency spectrum of phase current at (a) 10 rad/s, (b) 70 rad/s

B. Improved stator flux

The block digram of the compensation scheme is shown in Fig 9. All of the compensation and estimations were done within the software with sampling frequency of 55μs. Fig. 10 shows the simulation and experimental results of the stator flux before and after the compensation is applied with LP cut-off frequency of 5 rad/s and synchronous frequency of 31 rad/s. The waveforms of the stator flux from the simulation and experimental results clearly indicate the improvement in the stator flux after the compensation is applied. Fig 11 shows the waveforms of the referenece torque and actual torque obtained from simulation and experimental results before and after the compensation is applied. Due to the phase error present in the estimated stator flux, the actual torque before the compensation contain ripple at six times the fundamental frequency.

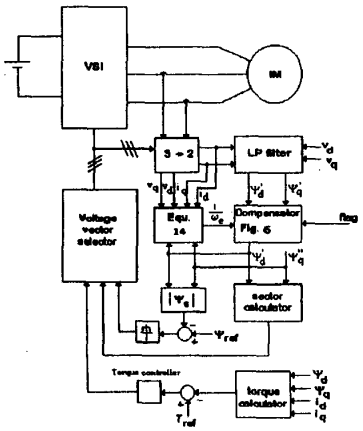

Fig. 9 Implementation of the compensation

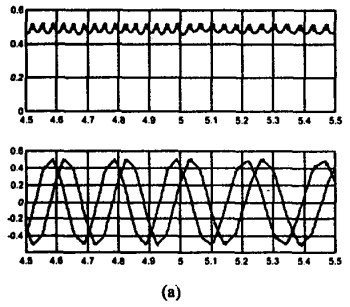

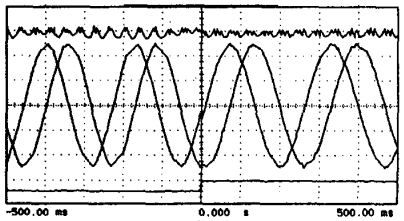

Fig. 10 Magnitude of the stator flux (top) d and q axis of stator flux (bottom), (a) simulation, (b) experiment

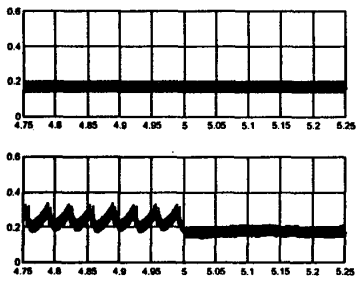

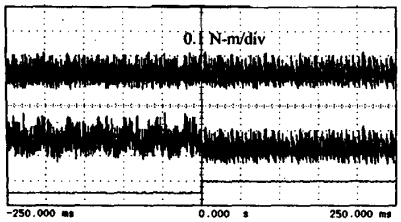

(b)

Fig. 11 Reference torque (upper trace) and actual torque (lower trace) obtained from (a) Simulation, (b) experiment

V. Conclusions

A constant switching frequency controller which replaces the conventional 3-level hysteresis comparator is introduced. It is shown by simulation and experiment that this controller has managed to maintain a constant switching frequency and reduces the torque ripple. The paper has also proposed a stator flux compensation technique which corrects the phase and magnitude errors in the estimated flux and hence reduces the ripple in the electromagnetic torque.

References

[1] Takahashi , T. Noguchi, "A new quick-response and high-efficiency control strategy of an induction motor", *IEEE Trans. Ind. Appl.*, vol IA-22, No 5 Sept/Oct 1986

[2] P. Tiitinen, "The next generation motor control method, DTC direct torque control", *Proc. of Int. Conf on Power Electronics, Drives and Energy System for Industrial Growth*, N. Delhi, India, pp. 37-43, 1996

[3] Y. Li, J. Shao,. and B. Si, "Direct torque control of induction motors for low speed drives considering discrete effect of control and dead-time timing of inverters", *in Conf. Rec. IEEE-IAS Annual Meeting*, pp. 781-788, 1997.

[4] J. K. Kang. and S. K. Sul, "Torque ripple minimisation strategy for direct torque control of induction motor", *in Conf. Rec. IEEE-IAS Annual Meeting*, pp. 438-443, 1998

[5] T. G. Habetler,. F. Profumo, M. Pastorelli and L. M. Tolbert, "Direct torque control of induction machines using space vector modulation", *IEEE Trans. Ind. Appl.*, Vol. 28, No. 5, pp. 1045-1053, 1992.

[6] I. G. Bird. and H. Zelaya De La Parra, "Fuzzy logic torque ripple reduction for DTC based AC drives", *Electronic Letters*, Vol. 33, No.17, pp. 1501-1502, 1997.

[7] S. Mir. and M. E. Elbuluk, "Precision torque control in inverter-fed induction machines using fuzzy logic", *In Conf. Rec. IEEE-IAS Annual Meeting*, pp. 396-401, 1995.

[8] D. Casadei, G. Grandi, G. Serra, A. Tani, "Effect of flux and torque hysteresis band amplitude in direct torque control of induction motor", *IECON '94*, , Bologna, Italy, 5-9 Sept 1994

[9] N.R.N. Idris, "Improved direct torque control of induction machines", *PhD Thesis*, Universiti Teknologi Malaysia, 2000.

[10] D. Casadei and G. Serra, "Analytical investigation of torque and flux ripple in DTC schemes for induction motors", in Proc. IEEE-IECON'97, pp. 552-556.